Received: 12 October 2021 | Revised: 21 December 2021 | Accepted: 22 December 2021

DOI: 10.1111/jnc.15571

Journal of Neurochemistry JNC The Official Journal of the International Society for Neurochemistry WILEY

ORIGINAL ARTICLE

Detection and quantification of Aβ–3–40 (APP669-711) in cerebrospinal fluid

Hans-Wolfgang Klafki[1] | Oliver Wirths[1] | Brit Mollenhauer[2,3] | Thomas Liepold[4] | Petra Rieper[1] | Hermann Esselmann[1] | Jonathan Vogelgsang[1] | Jens Wiltfang[1,5,6] | Olaf Jahn[1,4]

[1]Department of Psychiatry and Psychotherapy, University Medical Center Goettingen (UMG), Georg-August-University, Goettingen, Germany

[2]Department of Neurology, University Medical Center Goettingen (UMG), Georg-August-University, Goettingen, Germany

[3]Paracelsus-Elena-Klinik, Kassel, Germany

[4]Max Planck Institute of Experimental Medicine, Proteomics Group, Goettingen, Germany

[5]German Center for Neurodegenerative Diseases (DZNE), Goettingen, Germany

[6]Neurosciences and Signaling Group, Department of Medical Sciences, Institute of Biomedicine (iBiMED), University of Aveiro, Aveiro, Portugal

Correspondence
Hans-Wolfgang Klafki and Olaf Jahn, Department of Psychiatry and Psychotherapy, University Medical Center Goettingen (UMG), Georg-August-University, Von-Siebold-Str. 5, D37075 Goettingen, Germany.
Email: hans.klafki@med.uni-goettingen.de; olaf.jahn@med.uni-goettingen.de

Present address
Jonathan Vogelgsang, Department of Psychiatry, McLean Hospital, Harvard Medical School, Translational Neuroscience Laboratory, Belmont, Massachusetts 02478, USA

Abstract

Neurochemical biomarkers can support the diagnosis of Alzheimer's disease and may facilitate clinical trials. In blood plasma, the ratio of the amyloid-β (Aβ) peptides Aβ–3–40/Aβ1–42 can predict cerebral amyloid-β pathology with high accuracy (Nakamura et al., 2018). Whether or not Aβ–3–40 (aka. amyloid precursor protein (APP) 669–711) is also present in cerebrospinal fluid (CSF) is not clear. Here, we investigated whether Aβ–3–40 can be detected in CSF and to what extent the CSF Aβ–3–40/Aβ42 ratio is able to differentiate between individuals with or without amyloid-β positron emission tomography (PET) evidence of brain amyloid. The occurrence of Aβ–3–40 in human CSF was assessed by immunoprecipitation followed by mass spectrometry. For quantifying the CSF concentrations of Aβ–3–40 in 23 amyloid PET-negative and 17 amyloid PET-positive subjects, we applied a sandwich-type immunoassay. Our findings provide clear evidence of the presence of Aβ–3–40 and Aβ–3–38 in human CSF. While there was no statistically significant difference in the CSF concentration of Aβ–3–40 between the two diagnostic groups, the CSF Aβ–3–40/Aβ42 ratio was increased in the amyloid PET-positive individuals. We conclude that Aβ–3–40 appears to be a regular constituent of CSF and may potentially serve to accentuate the selective decrease in CSF Aβ42 in Alzheimer's disease.

KEYWORDS
Alzheimer's disease, biomarker, cerebrospinal fluid, immunoassay, immunoprecipitation, mass spectrometry

Abbreviations: AD, Alzheimer's disease; APP, amyloid precursor protein; AUC, area under the curve; Aβ, amyloid-β; BACE1, β-site APP cleaving enzyme 1; CHCA, 2-cyano-4-hydroxycinnamic acid; CNS, central nervous system; CSF, cerebrospinal fluid; DDM, n-dodecyl-β-D-maltoside; DMP, dimethyl pimelimidate dihydrochloride; IP, immunoprecipitation; IP-MS, immunoprecipitation followed by mass spectrometry; mAb, monoclonal antibody; MALDI-TOF-MS, matrix-assisted laser desorption/ionization time-of-flight mass spectrometry; NPH, normal pressure hydrocephalus; NTM, nonyl-β-D-thiomaltoside; PET, positron emission tomography; p-Tau, phospho Tau; ROC curve, receiver operating characteristic curve; RRID, Research Resource Identifier (see scicrunch.org); t-Tau, total Tau.

Jens Wiltfang and Olaf Jahn contributed equally.

1 | INTRODUCTION

Alzheimer's disease (AD) is a devastating neurodegenerative disorder with unmet medical need that is responsible for an estimated 60–80% of all cases of dementia (Alzheimer's Association, 2021). The characteristic neuropathological changes in AD brains, including cerebral accumulation of amyloid-β (Aβ) peptides and formation of neurofibrillary tangles, appear to precede the manifestation of clinical symptoms by many years (Jack et al., 2010; Price & Morris, 1999). Established biomarkers of AD neuropathology include increased signals on amyloid and tau positron emission tomography (PET) (Jagust, 2018) and measurements of soluble Aβ42, the Aβ42/Aβ40 ratio, total tau, and phosphorylated tau in cerebrospinal fluid (CSF) (Blennow & Zetterberg, 2018). Recent studies employing novel and highly sensitive assays indicate that, additionally, the measurements of particular phosphorylated forms of tau (Ashton et al., 2021; Janelidze et al., 2020; Karikari et al., 2020) and the concentration ratios of specific variants of Aβ in blood plasma (Kaneko, Nakamura, et al., 2014; Nakamura et al., 2018; Ovod et al., 2017; Shahpasand-Kroner et al., 2018) may serve as peripheral surrogate markers of AD-related pathological changes in the brain. Published mass spectrometry data indicate that CSF appears to contain primarily Aβ peptides starting at the aspartate residue in position one (Asp1) of the canonical Aβ amino acid sequence and with varying lengths of their carboxy-termini (Portelius et al., 2006, 2007; Portelius, Zetterberg, et al., 2006; Vigo-Pelfrey et al., 1993). In contrast, the pattern of Aβ variants in blood plasma seems to be more complex and includes a larger proportion of Aβ peptides with different amino-termini as indicated, for example, by a deviant isoelectric point on 2D-Western blot analysis (Maler et al., 2007).

In fact, more than 20 different Aβ-related proteolytic fragments of the amyloid precursor protein (APP) have been detected and identified in human blood plasma by immunoprecipitation followed by matrix-assisted laser desorption/ionization time-of-flight mass spectrometry (MALDI-TOF-MS) (Kaneko, Yamamoto, et al., 2014). These include a novel Aβ–3–40 (APP669–711) peptide which starts three amino acids N-terminal to the canonical Asp1 of the Aβ sequence. The ratio of Aβ–3–40/Aβ1-42 (APP669–711/Aβ1–42) in blood plasma and a composite biomarker calculated from the APP669–711/Aβ1–42 ratio plus the Aβ1–40/Aβ1–42 ratio were reported to represent novel and highly promising surrogate biomarkers of cerebral Aβ accumulation (Kaneko, Nakamura, et al., 2014; Nakamura et al., 2018). We have recently developed a sandwich immunoassay for the measurement of Aβ–3–40 in immunoprecipitates from human blood plasma and, in a small pilot study, observed a statistically significant reduction of the plasma Aβ42/Aβ–3–40 ratio in subjects with dementia of the Alzheimer's type as compared to other dementias (Klafki et al., 2020). The N-terminally elongated Aβ–3–40 can be generated by cultivated cells (Nakamura et al., 2018), and its cellular production does not seem to be reduced by inhibition of β-site APP cleaving enzyme 1 (BACE1) (Beyer et al., 2016; Portelius et al., 2013). While Aβ–3–x peptides gain increasing attention in the context of blood biomarker research for AD, it is still unclear whether these variants mainly originate from the periphery or the central nervous system, and whether they play a (pathological) role at the site of the disease in the brain. Knowledge on their occurrence in human CSF would be a first step to address these questions.

In the current study, we set out to explore whether Aβ–3–40 is also detectable in CSF. Using immunoprecipitation followed by MALDI-TOF-MS (IP-MS) we have obtained unequivocal evidence of the occurrence of Aβ–3–40 in pooled human CSF and in CSF samples from patients with normal pressure hydrocephalus (NPH). Next, we measured the CSF Aβ–3–40 concentrations in a small clinical sample dichotomized according to the results of amyloid PET. The CSF-concentrations of Aβ–3–40 as measured with our novel electrochemiluminescence sandwich immunoassay did not differ statistically significantly between amyloid PET-positive (n = 17) and amyloid PET-negative (n = 23) subjects. However, similar to the published findings in blood plasma (Kaneko, Nakamura, et al., 2014; Nakamura et al., 2018), we observed a statistically significant increase in the CSF Aβ–3–40/Aβ42 ratio in those patients with amyloid PET evidence of brain amyloid accumulation.

2 | MATERIALS AND METHODS

2.1 | Antibodies

The mouse monoclonal antibody (mAb) 6E10 was obtained from BioLegend, Cat. No SIG-39320 (Research Resource Identifier (RRID): AB_662798), mAb 14-2-4 from IBL International/Tecan (Hamburg, Germany), and mAb 101-1-1 from Biogenes GmbH (Berlin, Germany). MAb 14-2-4 and mAb 101-1-1 are directed against aminoterminally elongated Aβ–3–x and have been described in detail, previously (Klafki et al., 2020).

2.2 | Covalent coupling of monoclonal anti-Aβ antibodies to magnetic beads

Functionalized magnetic beads for immunoprecipitation were prepared by covalently coupling mAbs (clones 6E10, 14-2-4 or 101-1-1, see above) to Dynabeads M-270 Epoxy or Dynabeads M-280 Sheep anti-Mouse IgG (Cat. No. 14311 D and Cat. No. 11202 D, Invitrogen/ThermoFisher Scientific) according to the manufacturer's instructions. In the case of M-280 Sheep anti-Mouse IgG beads, covalent crosslinking with the anti-Aβ antibodies was achieved with dimethyl pimelimidate dihydrochloride (DMP) (Thermo Scientific, Cat. No. 21667).

2.3 | Cell culture

Transfected SH-SY5Y cells stably over-expressing wild-type APP695 carrying an amino-terminal Myc tag and a carboxy-terminal Flag tag (Munter et al., 2010) (kindly provided by L. Münter and G. Multhaup) were cultured at 37°C, 5% CO_2 in D-MEM/F12, supplemented with

10% fetal calf serum, 2 mM L-glutamine, non-essential amino acids, and 500 μg/ml hygromycin B (Haussmann et al., 2013). The cell line (SH-SY5Y) is not listed as a commonly misidentified cell line by the International Cell Line Authentication Committee (https://iclac.org/databases/cross-contaminations/). The cell line was not further authenticated in the laboratory. The maximum number of passages after thawing from cryopreservation was six.

2.4 | Detection of Aβ−3–40 in cell culture supernatant and human CSF by immunoprecipitation and MALDI-TOF-MS

For pre-concentration of some of the samples (see below), Amicon Ultra 2 ml centrifugal filters with Ultracell-3K membrane (Cat. No. UFC200324, Millipore Corporation) or Vivaspin 3000 MWCO PES spin filters (6 ml (Cat. No. VS0691) or 20 ml (Cat. No. VS2091), Sartorius Goettingen Germany) were used. The protocol for immunoprecipitation followed by mass spectrometry (IP-MS) was essentially based on the IP-MS method described by Nakamura and colleagues (Nakamura et al., 2018) and included two consecutive rounds of IP. A volume of 500 μl of cell culture supernatant or CSF (with or without pre-concentration and, if applicable, volume adjustment by subsequent addition of H_2O) was mixed with an equal volume of 100 mM Tris-HCl, pH 7.4 containing 0.2% (w/v) nonyl-β-D-thiomaltoside (NTM) and 0.2% (w/v) n-dodecyl-β-D-maltoside (DDM). Next, 30 μl of Dynabeads M-280-6E10 were added, and the mixture was incubated overnight at approximately 4°C or for 1 h at approximately 20°C with continuous shaking. After five washes with 50 mM Tris-HCl, pH 7.4, 150 mM NaCl, 0.1% (w/v) DDM, 0.1% (w/v) NTM, Aβ peptides were eluted 2 × 5 min at approximately 20°C and 800 RPM on a shaker with 2 × 15 μl of 50 mM glycine/HCl, pH 2.8 containing 0.1% (w/v) NTM. The eluates were combined (total volume: 30 μl per sample) and mixed with 220 μl of H_2O, 250 μl of 100 mM Tris-HCl, pH 7.4 containing 0.2% (w/v) NTM and 0.2% (w/v) DDM and 15 μl of functionalized magnetic Dynabeads M-270 Epoxy coupled to mAb 6E10, mAb 14–2–4, or mAb 101–1–1. After 60-min incubation on a shaker at approximately 20°C, the magnetic bead-immune complexes were washed five times with 50 mM Tris-HCl, pH 7.4, 150 mM NaCl, 0.1% (w/v) DDM, 0.1% (w/v) NTM, resuspended in 500 μl of 50 mM ammonium acetate (pH approximately 7.0) and directly subjected to sample preparation for mass spectrometric analysis. For this purpose, the beads were immobilized on a magnetic rack and the supernatant was removed, followed by one additional wash with 50 mM ammonium acetate and one with H_2O. Care was taken to quantitatively remove residual H_2O prior to eluting the Aβ peptides in 2.5 μl of 70% acetonitrile containing 5 mM HCl. The eluates (0.5 μl) were spotted onto a prestructured MALDI sample support (MTP AnchorChip 384 BC; Cat. No. 8280790, Bruker, Bremen, Germany) without prior precoating of the hydrophilic anchor spots with matrix. Instead, 0.5 μl matrix solution consisting of 5 mg/ml 2-cyano-4-hydroxycinnamic acid (CHCA, Cat. No. 70990-1G-F, Sigma Aldrich/Merck, Taufkirchen, Germany) in 50% acetonitrile/0.05% trifluoroacetic acid was added to each sample droplet. Calibrant spots were prepared in the same way with 0.5 μl of a 1:1 mixture of the peptide standards Peptide Calibration Standard II (Cat. No. 8222570, Bruker, Bremen, Germany) and PepMix2 (Cat. No. C102, LaserBio Labs, Valbonne, France), providing a calibrant range of up to 6000 mass-to-charge (m/z). After drying, the samples were introduced into an ultrafleXtreme MALDI-TOF/TOF mass spectrometer operated under the software flexControl 3.4 (Bruker, Bremen, Germany). For mass spectrometric analysis of Aβ peptides, positively charged ions in the m/z range of 1800–6000 were first recorded in the reflector mode to generate high-resolution mass spectra, from which accurate monoisotopic masses could be derived (at the cost of sensitivity). Subsequently, the instrument was switched into the linear mode where laser energy was increased by 30–40% and detector voltage by 20–30% compared to the reflector mode settings. The resulting low-resolution mass spectra provided average masses with increased intensity (at the cost of mass accuracy). In both acquisition modes, a total of 5000 spectra per sample were recorded from different spot positions and the software flexAnalysis 3.4 (Bruker) was used to annotate and calibrate monoisotopic masses with the implemented SNAP2 algorithm and cubic calibration, while centroiding and quadratic calibration was used for average masses.

2.5 | Study approval and study cohort

The study was conducted with archived CSF samples from the biobank of the Department of Psychiatry and Psychotherapy, University Medical Center Goettingen. The pseudonomized collection of biological samples and clinical data and their use in biomarker studies was approved by the ethics committee of the University Medical Center Goettingen (9/2/16). All subjects or their legal representatives gave their informed consent prior to inclusion. The study was not preregistered and no blinding was performed. The study was exploratory. No tests for outliers were performed. The study participants were classified into the groups amyloid PET-negative and amyloid PET-positive according to amyloid PET with ^{18}F Florbetaben or ^{18}F Florbetapir. The clinical sample (n = 40) included 38 subjects that have been described in detail in a recent biomarker study (Aichholzer et al., 2021). In the context of that study, CSF Aβ38, Aβ40, and Aβ42 had been determined with the V-Plex Aβ panel 1 (6E10) multiplex assay kit (Meso Scale Discovery, Cat. No. K15200E) in 16-fold diluted samples. CSF data regarding total Tau (t-Tau) and phospho Tau 181 (p-Tau) were obtained from routine measurements in the laboratory of Clinical Chemistry, University Medical Center Goettingen (ibid.). The characteristics of the study cohort are summarized in Table 1. Control CSF sample pools were prepared by combining several CSF samples from the local biobank in Goettingen (see above) or archived CSF samples that had been collected earlier within the study of the German Dementia Competence Network (DCN, recruitment period: 2003–2007) (Kornhuber et al., 2009; Lewczuk et al., 2006) at site Goettingen (ethical approval: 40/7/02). Additional control CSF samples from participants with normal pressure hydrocephalus (NPH) were collected as part of the "Kassel cohort" at Paracelsus-Elena-Klinik,

TABLE 1 Characteristics of the study cohort and baseline statistics of CSF measurements[a]

	Amyloid PET-negative ($n = 23$)	Amyloid PET-positive ($n = 17$)	p-value amyloid PET-positive vs. -negative
Age [years, mean ± SD]	65.52 ± 11.42	68.29 ± 11.20	0.4488[b] ($t = 0.7654$, df = 38)
Gender			0.7471[c]
Women	10 (43.5%)	6 (35.3%)	
Men	13 (56.5%)	11 (64.7%)	
APOE genotype			
ε2/ε2	–	–	
ε2/ε3	3	–	
ε2/ε4	1	1	
ε3/ε3	14	7	
ε3/ε4	4	8	
ε4/ε4	1	1	
≥1 *APOE* ε4 allele, *n* (%)	6 (26.1%)	10 (58.8%)	0.0531[c]
CSF p-Tau[e] [pg/ml, mean ± SD]	57.57 ± 37.77	69.76 ± 27.39	0.0633[d] (U = 127.5)
CSF t-Tau[e] [pg/ml, mean ± SD]	412.2 ± 366.5	578.0 ± 339.1	0.0392[d] (U = 120)
CSF Aβ38 [pg/ml, mean ± SD]	2941 ± 1111	2509 ± 734.8	0.2537[d] (U = 153)
CSF Aβ40 [pg/ml, mean ± SD]	9699 ± 3748	8343 ± 2575	0.2315[d] (U = 151)
CSF Aβ42 [pg/ml, mean ± SD]	856.5 ± 463.6	441.2 ± 157.3	0.0001[d] (U = 61)
CSF ratio Aβ42/Aβ40 [mean ± SD]	0.0866 ± 0.0193	0.0543 ± 0.0195	<0.0001[d] (U = 49)

[a]For 38 of the 40 study participants, the demographical data, ApoE genotype and cerebrospinal fluid (CSF) measurements of Aβ38, Aβ40, Aβ42, p-Tau, and t-Tau have been published before (Aichholzer et al., 2021).

[b]Unpaired two-tailed *t*-test.

[c]Two-sided Fisher's exact test, or

[d]Two-tailed Mann–Whitney test for differences between the diagnostic groups.

[e]The CSF concentrations of p-Tau and t-Tau were measured routinely in the laboratory of Clinical Chemistry, University Medical Center Goettingen. According to the respective cutpoints, CSF concentrations of p-Tau >61 pg/ml and of t-Tau >450 pg/ml are considered abnormal. *n* = number of patients in the diagnostic groups.

Kassel, Germany (ethical vote 09/07/04 and FF 38/2016). Biomaterial sampling and data collection was conducted according to the revised Declaration of Helsinki and good clinical practice guidelines.

2.6 | Quantification of Aβ–3–40 in human CSF

The Aβ–3–40 concentrations in human CSF samples were measured with a chemiluminescence sandwich immunoassay we have developed and described in detail, recently (Klafki et al., 2020). In the final assay protocol applied in this study, the CSF samples were removed from storage at −80°C, thawed and diluted four-fold with Diluent-35 (Meso Scale Discovery, Cat. No R50AE) prior to the measurements in two technical replicates on the same assay plate.

2.7 | Statistical analysis

Statistical analyses were done with IBM SPSS Statistics 26 and GraphPad Prism 9. No sample size calculation was performed prior to the Aβ measurements. The sample size was estimated on the basis of previous studies of similar nature (Aichholzer et al., 2021; Klafki et al., 2020). For post hoc power validation, we used G*Power 3.1.9.7 (Faul et al., 2007). No tests for outliers were performed. No exclusion criteria were predetermined. To test for normal distribution of continuous variables, Shapiro–Wilk test was employed. For group comparisons of normally distributed continuous variables, we used unpaired two-tailed *t*-test and for non-normally distributed variables two-tailed Mann–Whitney test. *p*-values <0.05 were considered statistically significant. For assessing the diagnostic potential of single biomarker candidates and for the combination of the CSF ratios Aβ–3–40/Aβ42 and Aβ42/Aβ40 (combined biomarker candidate, composite biomarker), the predicted probabilities of amyloid positivity were calculated by binary logistic regression with IBM Statistics SPSS 26. The resulting values were then further used for calculating receiver operating characteristic (ROC) curves.

3 | RESULTS

3.1 | Experimental workflow and study cohort

A flowchart summarizing the methods and samples that were used for the identification and quantification of Aβ–3–40 in the different parts of this study is presented in Figure S1. In line with its definition, the

amyloid PET-positive group showed a typical AD amyloid PET pattern. Demographically, the amyloid PET-positive group was slightly older (68.3 vs. 65.5 years) and contained 64.7% males, while there were only 56.5% males in the amyloid PET-negative group (Table 1). Clinically, the amyloid PET-positive group had a slightly lower MMSE (24.1) compared to the amyloid PET-negative group (25.1) and a higher clock drawing test score of 2.4 versus 2.2. None of the demographic or clinical differences reached our predefined significance level of 0.05. Clinical diagnoses were based on the ICD-10 coding system. The amyloid PET-positive group were mainly Alzheimer's dementia or MCI because of Alzheimer's disease, however, very few (3 of 17 patients) were clinically diagnosed as major depressive disorder since these patients did not fulfill the clinical criteria of MCI or dementia. Diagnostically, the amyloid PET-negative patients were much more heterogeneous. Clinical diagnoses were affective disorders, substance abuse, MCI not because of AD or other dementia, for example, Lewy Body dementia, vascular dementia, or other unspecified dementia.

3.2 | Detection of Aβ−3−40 in human CSF by IP-MS

To provide objective evidence of the presence of Aβ−3−40 in human CSF, we applied a modification in the IP-MS method developed by Nakamura and colleagues (Nakamura et al., 2018) including two consecutive rounds of magnetic bead IP. In the first IP-round, we employed Dynabeads M-280 Sheep anti-Mouse IgG covalently functionalized with mAb 6E10 which recognizes several N-terminal Aβ-variants (Klafki et al., 2020) and APP (Knobloch et al., 2007; Lord et al., 2006). In the subsequent second IP-round, Dynabeads M-270 Epoxy covalently coupled to mAb 6E10, mAb 14−2−4 or mAb 101−1−1 were used. The latter two antibodies were raised against the amino-terminus of Aβ−3−x and have been characterized in detail in a previous study (Klafki et al., 2020). In a pilot experiment, employing conditioned cell culture supernatant of SH-SY5Y cells over-expressing human wild-type APP695, we compared overnight incubation at approximately 4°C in the first IP round versus 1 h at approximately 20°C. The subsequent second IP round was carried out for 1 h at approximately 20°C in all cases. Mass spectrometric analysis indicated that overnight incubation at approximately 4°C in the first IP round resulted in an overall higher signal intensity for Aβ peptides as compared to a 1-h incubation at approximately 20°C (Figure 1, Figure S2). Notably, Aβ−3−40 was detected only as a very small peak when the pan-specific anti-Aβ antibody mAb 6E10 was used in both IP rounds (Figure 1, Figure S2). Replacing mAb 6E10 in the second IP round by mAb 14−2−4 or 101−1−1 reduced the signals corresponding to Aβ variants starting with Asp1 and considerably improved the detection of Aβ−3−40 (Figure 1, Figure S2). Additionally, Aβ−3−38 was found. The Aβ variants detected reliably in the cell culture supernatant by this IP-MS approach are summarized in Table 2.

In the next step, we explored whether Aβ−3−40 was also present in human CSF. Indeed, the Aβ−3−40 peptide was clearly detected in a pooled lumbar CSF sample after overnight IP with M-280-6E10 beads (first IP-round) followed by a second IP with mAb 14−2−4 or 101−1−1 coupled to M-270 Epoxy beads (Figure 2). Additionally, a smaller peak at m/z 4491 corresponding to Aβ−3−38 was visible when mAb14-2−4 was used in the second IP round (Figure 2a). These results were confirmed in an independent pooled lumbar CSF sample with M-270−14−2−4 magnetic beads in the second IP-round (Figure 2b, mass spectrum I). The signal intensities were increased, particularly for Aβ−3−40 and Aβ−3−38, when the pooled CSF was pre-concentrated via centrifugal filtration (Figure 2b, mass spectrum II).

Similar profiles of Aβ variants were observed in NPH-CSF samples with M-270−14−2−4 or M-270−101−1−1 magnetic beads employed in the second IP-round (Figure S3), further corroborating the presence of Aβ−3−40 and Aβ−3−38 in CSF, independent of input material and antibody used. The Aβ variants detected reliably in CSF by our IP-MS approach are summarized in Table 3. Taken together, our findings provide strong evidence of the regular occurrence of Aβ−3−40 in human CSF.

When comparing the IP-MS results from different CSF sources, we noted a high variability in the co-immunoprecipitation of Aβ variants starting at Asp1 with both tested antibody combinations employing either mAb 14−2−4 or mAb 101−1−1 in the second IP-round. In some experiments, Aβ1−40 even represented the most prominent signal in the recorded mass spectra. However, we also observed the other extreme with Aβ−3−40 being the dominant signal, while Aβ1−40 was barely detectable (see for example Figure S3a). The reason why the use of mAb 14−2−4 and mAb 101−1−1 in the second IP-round led to such a fluctuation in the extent of co-immunoprecipitation of Aβ1−x peptides has not been clarified, yet. At least, it can be excluded that this effect was antibody-dependent (both mAb 14−2−4 and mAb 101−1−1 showed it) and that it was CSF-specific, as we observed a similar fluctuation also with cell culture supernatants (data not shown). It might be related to the experimental conditions during the two-step IP procedure, including elution after the first IP under acidic and thereby potentially aggregation-promoting conditions. Notably, mAb 14−2−4 and mAb 101−1−1 can recognize the N-terminally elongated Aβ−3−40 peptide with very strong preference over Aβ1−40 on Western blot, capillary isoelectric focusing (CIEF)-immunoassay and electrochemiluminescence sandwich immunoassay (see: Ref. (Klafki et al., 2020) and Figure S4). For the reasons mentioned, we refrained from using the two-step IP-MS procedure for quantification purposes, which would have required a more sophisticated protocol with a stable isotope-labeled Aβ−3−40 standard. After having proven its identity in CSF mass spectrometrically, we instead chose to quantify Aβ−3−40 from CSF without prior enrichment using our established electrochemiluminescence sandwich immunoassay.

3.3 | Quantification of Aβ−3−40 in human CSF samples

Next, we measured the CSF concentration of Aβ−3−40 in human CSF with a highly selective electrochemiluminescence sandwich

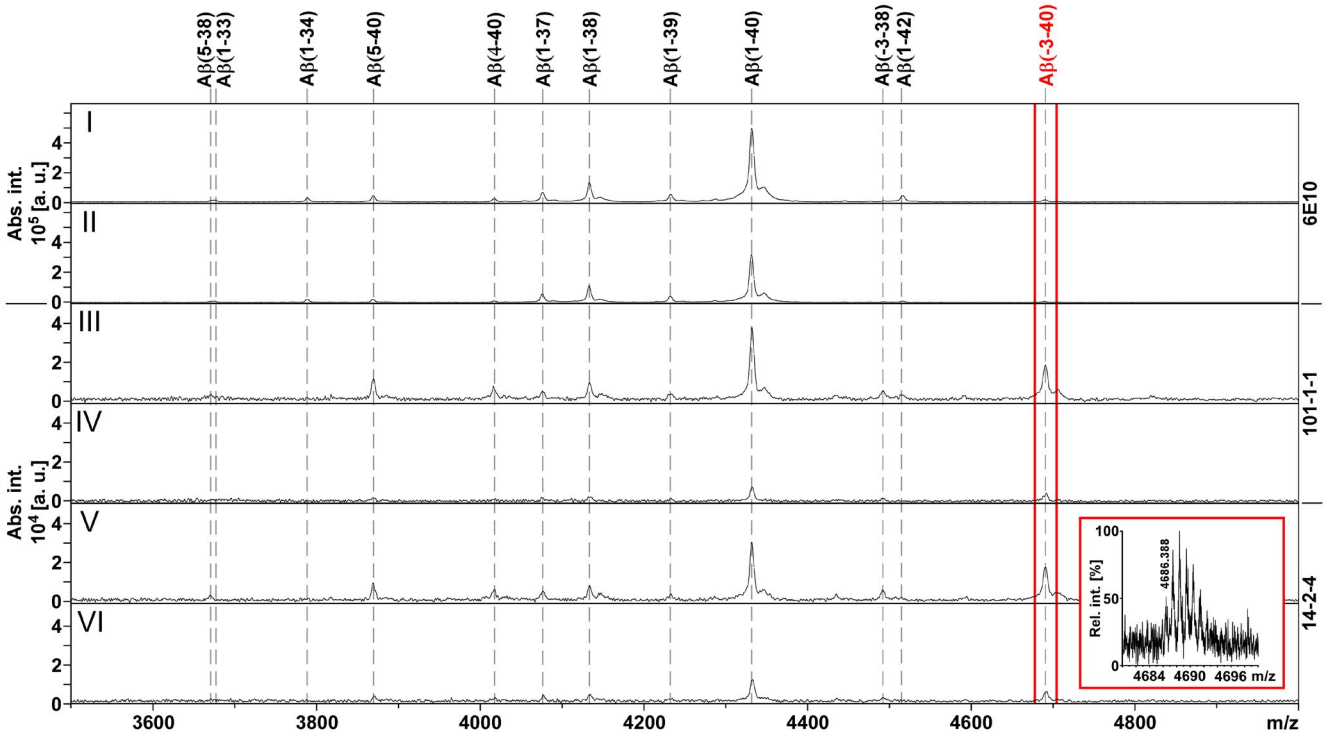

FIGURE 1 MALDI-TOF-MS mass spectra of immunoprecipitated Aβ peptides from cell culture supernatant. Aliquots of conditioned cell culture medium of SH-SY5Y cells over-expressing human amyloid precursor protein (APP695) were subjected to two consecutive rounds of magnetic bead immunoprecipitation (IP) and analyzed by matrix-assisted laser desorption/ionization time-of-flight mass spectrometry (MALDI-TOF-MS). In the first IP-round, the samples were incubated with monoclonal antibody (mAb) 6E10 covalently coupled to Dynabeads-M-280 Sheep anti-Mouse IgG overnight at approximately 4°C (mass spectra I, III, V) or for 1 h at approximately 20°C (II, IV, VI). In the second IP-round (1 h at approximately 20°C), Dynabeads M-270 Epoxy functionalized with mAb 6E10 (I, II), mAb 101–1–1 (III, IV), or mAb 14–2–4 (V, VI) were employed. Note the different scaling of the intensity axis in I and II versus III-VI. Linear mode mass spectra are shown with annotations of the respective amyloid-β (Aβ) peptides on top. The signals for Aβ–3–40 are highlighted in red. The insert shows the isotopic resolution of the Aβ–3–40 signal as derived from the corresponding reflector mode MALDI-TOF-MS mass spectra shown in Figure S2. Accordingly, Aβ–3–40 was detected with a relative mass deviation of only 6.0 ppm ($[M+H]^+_{mono,\ calc}$ = 4686.360, $[M+H]^+_{mono,\ obs}$ = 4686.388). In general, Aβ variants were assigned to the respective signals only when confirmed by accurate mass information from reflector mode mass spectra

immunoassay we have developed in house and validated thoroughly in a previous study (Klafki et al., 2020). To determine a suitable dilution factor for the CSF measurements, we first tested four different control CSF samples from our local biobank after 2-fold, 3-fold, 4-fold, 6-fold, and 8-fold dilution in Diluent-35. The recorded signals decreased with increasing sample dilution, as expected (Figure 3a). Plotting the dilution-corrected Aβ–3–40 CSF concentrations against the dilution factor indicated that fourfold sample dilution was sufficient to ameliorate potential matrix interferences and, at the same time, allowed for recording Aβ–3–40 signals in the detection range of the assay (Figure 3b).

Using the assay conditions established, CSF samples from 23 amyloid PET-negative and 17 amyloid PET-positive subjects were measured after 4-fold dilution with Diluent-35. All 40 CSF measurements were in the detection range of the assay (i.e., signals above the lower limit of detection [LLOD]). Furthermore, 39 of the 40 samples (97.5%) produced signals above the lower limit of quantification (LLOQ, defined as 10 × SD above lowest standard / zero calibrator). The calculated Aβ–3–40 concentrations in the CSF samples were normally distributed in the amyloid PET-positive but not in the amyloid PET-negative subjects (Table S1). There was no statistically significant difference in the Aβ–3–40 CSF concentrations between the diagnostic groups (Figure 4a).

3.4 | Assessment of the CSF Aβ–3–40/Aβ42 ratio as a novel biomarker candidate of cerebral amyloid deposition

To calculate the CSF Aβ42/Aβ–3–40 ratio and the inverse Aβ–3–40/Aβ42 ratio, the current measurements of CSF Aβ–3–40 (measured in 4-fold diluted CSF-samples) and already existing data on the CSF levels of Aβ40 and Aβ42 determined with the MSD Aβ Panel 1 (6E10) multiplex assay kit after 16-fold sample dilution were used. For n = 38 of the 40 subjects included in the current study, the CSF concentrations of Aβ38, Aβ40, Aβ42, and the Aβ42/Aβ40 ratios have been published before (Aichholzer et al., 2021).

TABLE 2 Aβ variants in supernatant of cultivated SH-SY5Y APP695 cells detected by IP-MS[b]

Aβ variant	$[M+H]^+_{mono, calc}$	$[M+H]^+_{mono, obs}$	$[M+H]^+_{avg, calc}$	$[M+H]^+_{avg, obs}$
Aβ−3–40	4686.360	4686.339–4686.486 (4)	4689.32	4690.58–4691.58 (4)
Aβ1–42	4512.277	4512.108–4512.284 (2)	4515.05	4515.96–4516.08 (2)
Aβ−3–38	4488.223	4488.211–4488.356 (2)	4491.06	4491.80–4492.13 (2)
Aβ1–40	4328.156	4328.016–4328.284 (6)	4330.82	4331.36–4332.43 (6)
Aβ1–39	4229.087	4228.952–4229.147 (2)	4231.69	4232.09–4232.55 (2)
Aβ1–38	4130.019	4129.873–4130.075 (4)	4132.56	4132.93–4133.49 (4)
Aβ1–37	4072.997	4072.862–4073.127 (4)	4075.50	4075.87–4076.74 (4)
Aβ4–40	4013.049	4012.885–4013.119 (4)	4015.54	4016.01–4017.28 (4)
Aβ5–40	3865.981	3865.848–3866.057 (4)	3868.36	3868.57–3869.34 (4)
Aβ1–34	3785.867	3785.747–3785.922 (2)	3788.13	3788.46–3788.70 (2)
Aβ1–33	3672.783	3672.689–3672.854 (2)	3674.97	3673.11–3675.19 (2)
Aβ5–38	3667.844	3667.735–3667.979 (2)	3670.10	3670.29–3670.32 (2)

[a]The listed peptides were detected in at least two independent mass spectra. Assignment was based on accurate mass information from reflector mode mass spectra. $[M+H]^+_{mono, calc}$, theoretical m/z of the singly charged monoisotopic mass; $[M+H]^+_{mono, obs}$, observed m/z of the singly charged monoisotopic mass, given as range with number of detections in parentheses; $[M+H]^+_{avg, calc}$, theoretical m/z of the singly charged average mass; $[M+H]^+_{avg, obs}$, observed m/z of the singly charged average mass, given as range with number of detections in parentheses. Aβ, amyloid-β; APP, amyloid precursor protein; IP-MS, immunoprecipitation followed by mass spectrometry.

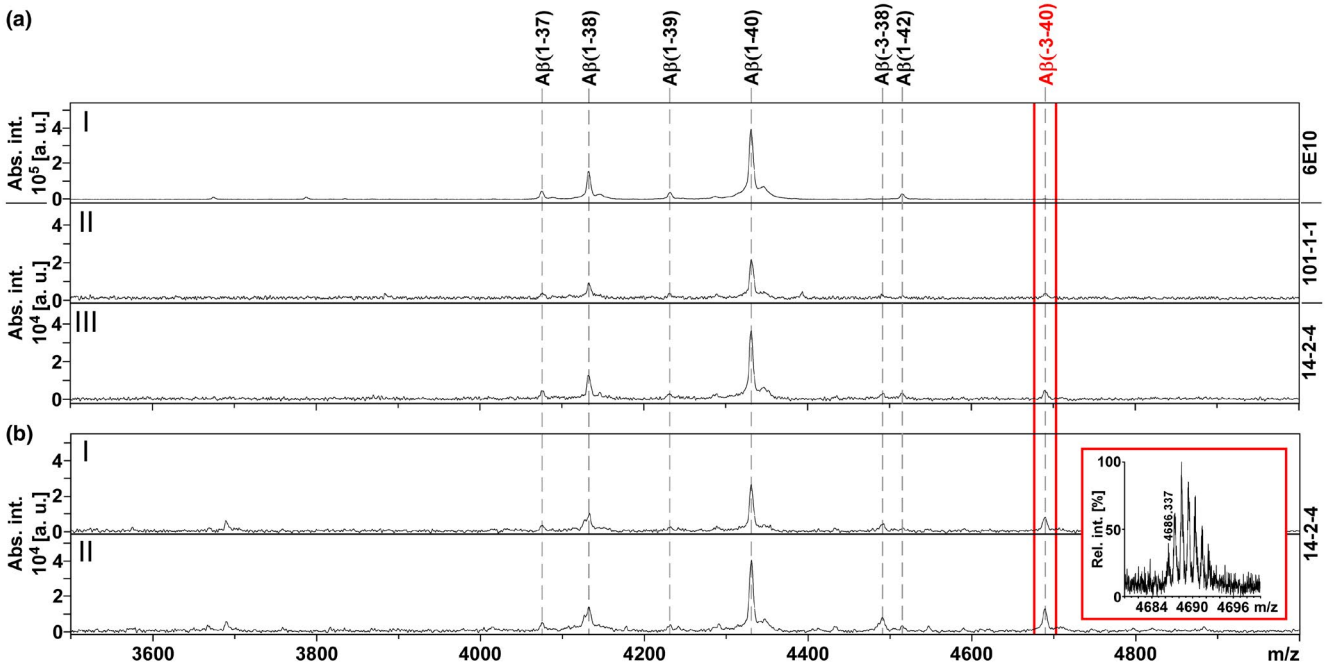

FIGURE 2 MALDI-TOF-MS mass spectra of immunoprecipitated Aβ peptides from pooled lumbar CSF. Aliquots of pooled cerebrospinal fluid (CSF) (prepared from several individual CSF samples) were subjected to two consecutive rounds of magnetic bead immunoprecipitation (IP) and analyzed by matrix-assisted laser desorption/ionization time-of-flight mass spectrometry (MALDI-TOF-MS). In the first IP-round, the samples were incubated with monoclonal antibody (mAb) 6E10 covalently coupled to Dynabeads M-280 anti-mouse IgG overnight at approximately 4°C. In the second IP-round (1 h at approximately 20°C), Dynabeads M-270 Epoxy functionalized with mAb 6E10 (a, mass spectrum I), mAb 101–1–1 (a, II) or mAb 14–2–4 (a, III) were employed. Note the different scaling of the intensity axis in I versus II and III. Applying the same procedure (second IP-round with mAb 14–2–4) to an independent pooled CSF sample without (b, mass spectrum I) and with (b, II) pre-concentration (approximately 5-fold) confirmed the previous result (a, mass spectrum III). Linear mode mass spectra are shown with annotations of the respective amyloid-β (Aβ) peptides on top. The signals for Aβ−3–40 are highlighted in red. The insert shows the isotopic resolution of the Aβ−3–40 signal as derived from the corresponding reflector mode MALDI-TOF-MS mass spectra. Accordingly, Aβ−3–40 was detected with a relative mass deviation of only 4.9 ppm ($[M+H]^+_{mono, calc}$ = 4686.360, $[M+H]^+_{mono, obs}$ = 4686.337). In general, Aβ variants were assigned to the respective signals only when confirmed by accurate mass information from reflector mode mass spectra (not shown)

TABLE 3 Detection of Aβ variants in CSF by IP-MS[c]

Aβ variant	$[M+H]^+_{mono, calc}$	$[M+H]^+_{mono, obs}$	$[M+H]^+_{avg, calc}$	$[M+H]^+_{avg, obs}$
Aβ−3–40	4686.360	4686.337–4686.684 (7)	4689.32	4689.17–4690.47 (7)
Aβ1–42	4512.277	4512.342–4512.520 (2)	4515.05	4515.33–4515.42 (2)
Aβ−3–38	4488.223	4488.230–4489.408 (7)	4491.06	4490.66–4492.37 (7)
Aβ1–40	4328.156	4328.150–4328.375 (8)	4330.82	4330.53–4331.47 (8)
Aβ1–39	4229.087	4228.634–4229.192 (2)	4231.69	4231.67–4232.05 (2)
Aβ1–38	4130.019	4130.057–4130.186 (6)	4132.56	4132.25–4132.91 (6)
Aβ1–37	4072.997	4073.091–4073.260 (2)	4075.50	4075.30–4075.61 (2)

[a]The listed peptides were detected in at least two independent mass spectra. Assignment was based on accurate mass information from reflector mode mass spectra. $[M+H]^+_{mono, calc}$, theoretical m/z of the singly charged monoisotopic mass; $[M+H]^+_{mono, obs}$, observed m/z of the singly charged monoisotopic mass, given as range with number of detections in parentheses; $[M+H]^+_{avg, calc}$, theoretical m/z of the singly charged average mass; $[M+H]^+_{avg, obs}$, observed m/z of the singly charged average mass, given as range with number of detections in parentheses. Aβ, amyloid-β; IP-MS, immunoprecipitation followed by mass spectrometry.

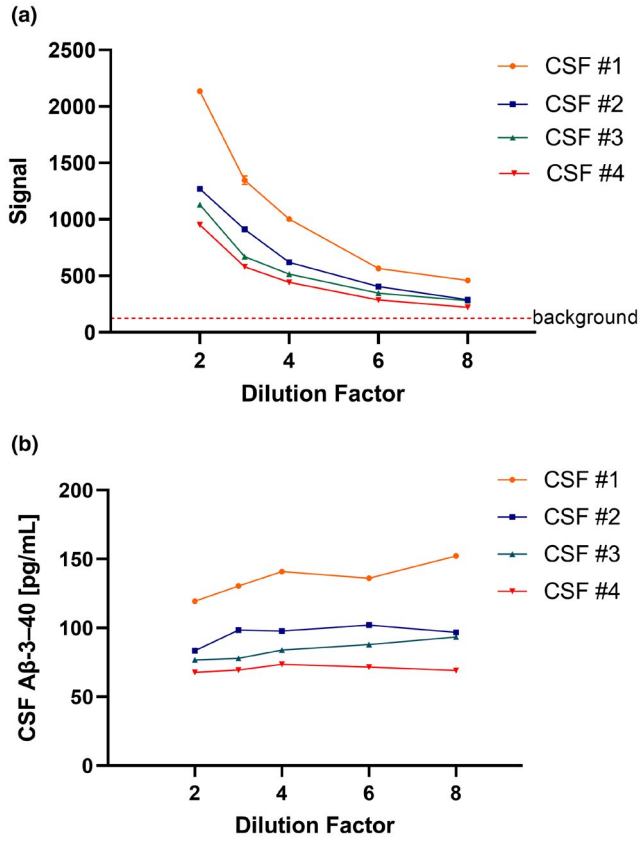

FIGURE 3 Impact of sample dilution on the measurement of Aβ−3–40 in human CSF. Four different individual cerebrospinal fluid (CSF) samples were measured with the amyloid-β (Aβ)−3–40 assay after two, three, four, six, and eightfold dilution with Diluent-35. The recorded signals (a) and dilution-corrected, calculated CSF concentrations (b) of Aβ−3–40 were plotted against the respective dilution factors. Based on these observations, 4-fold sample dilution was selected for further CSF measurements

The CSF Aβ−3–40/Aβ42 ratio followed Gaussian distribution in amyloid PET-negative and amyloid PET-positive subjects, but not the inverse Aβ42/Aβ−3–40 ratio (Table S1). This observation was in agreement with published IP-MS findings regarding the APP669–711 (Aβ−3–40)/Aβ1–42 ratio in blood plasma (Kaneko, Nakamura, et al., 2014; Nakamura et al., 2018). Consequently, we proceeded with the CSF Aβ−3–40/Aβ42 ratio for further statistical evaluation.

The mean CSF Aβ−3–40/Aβ42 ratio was statistically significantly higher in the amyloid PET-positive subjects than in the amyloid PET-negative cases (Figure 4b).

3.5 | Comparison of selected single and combined biomarker candidates for identifying amyloid positivity

The predicted probability of amyloid positivity was calculated by binary logistic regression for CSF Aβ42, the Aβ−3–40/Aβ42 ratio, the Aβ42/Aβ40 ratio and for a model including both, the CSF Aβ−3–40/Aβ42 and the $Aβ_{42}/Aβ_{40}$ ratio (combined biomarker). The resulting values (predicted probabilities) were then further used for calculating receiver operating characteristic (ROC) curves (Figure 5). The areas under the ROC curves (AUCs) for identifying amyloid PET-positivity were 0.844 for CSF Aβ42, 0.867 for the CSF Aβ−3–40/Aβ42 ratio, 0.873 for the Aβ42/Aβ40 ratio, and 0.880 for a model including both ratios, CSF Aβ−3–40/Aβ42 and Aβ42/Aβ40.

4 | DISCUSSION

Surrogate biomarkers of the neuropathological changes in AD brains can support the early and differential diagnosis of neurodegenerative disorders and may serve for improved cohort selection for clinical trials and, potentially, monitoring target engagement and treatment response (Alawode et al., 2021; Cummings, 2019). Recently, the blood plasma concentration ratios of Aβ42/Aβ40 (Ovod et al., 2017; Schindler et al., 2019), Aβ1–40/Aβ1–42, and Aβ−3–40/Aβ1–42 (a.k.a. APP669-711)/Aβ1-42) were discovered to represent novel and highly accurate peripheral biomarkers of cerebral Aβ accumulation (Kaneko, Nakamura, et al., 2014; Nakamura et al., 2018). Since blood is easily accessible, blood biomarker tests have clear and obvious

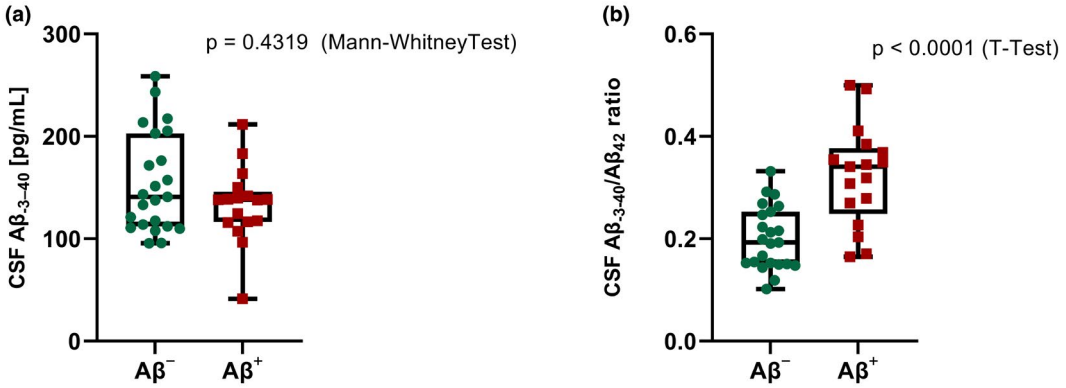

FIGURE 4 CSF Aβ–3–40 levels and CSF Aβ–3–40/Aβ42 ratios in amyloid PET-negative ($A\beta^-$) and amyloid PET-positive ($A\beta^+$) subjects. (a) The measured cerebrospinal fluid (CSF) concentrations (corrected for sample dilution) of CSF amyloid-β (Aβ)–3–40 and box plots with medians and min – max whiskers are shown. There was no statistically significant difference between amyloid positron emission tomography (amyloid PET)-negative ($n = 23$) and amyloid PET-positive subjects ($n = 17$) (two-tailed Mann–Whitney test, $p = 0.4319$, $U = 166$). (b) The Aβ–3–40/Aβ42 ratios in CSF were higher in the amyloid PET-positive cases ($p < 0.0001$, two-tailed unpaired t-test, $t = 4.848$, df = 38). Post hoc power analysis for the two-tailed unpaired t-test (difference between the mean Aβ–3–40/Aβ42 ratios in the two groups) indicated an achieved power (1–β) of 0.997 ($\alpha = 0.05$, effect size $d = 1.55147$, $n_1 = 23$, $n_2 = 17$, $\mu_1 = 0.2009$, $\mu_2 = 0.3231$, $SD_1 = 0.06136$, $SD_2 = 0.09776$, pooled SD (weighted) = 0.078764, Df = 38, noncentrality parameter δ = 4.8507, critical $t = 2.02439$)

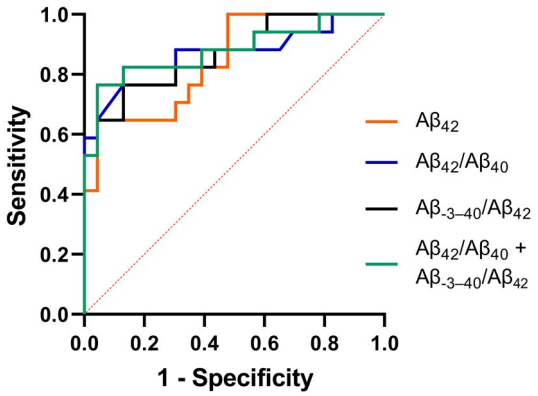

FIGURE 5 Receiver operating characteristic (ROC) curves of single and combined biomarker candidates for the discrimination between amyloid PET-negative and amyloid PET-positive subjects. The predicted probabilities of amyloid positron emission tomography (amyloid PET)-positivity were first calculated by binary logistic regression for amyloid-β (Aβ)42, the Aβ42/Aβ40 ratio, the Aβ–3–40/Aβ42 ratio and a model including both, the Aβ42/Aβ40 and the Aβ–3–40/Aβ42 ratio. In the next step, the resulting values were used for receiver operating characteristic (ROC) curve calculations. The areas under the curves (AUCs) were 0.844 for CSF Aβ42 (95% confidence interval (95% CI): 0.723–0.965, orange line), 0.867 for the cerebrospinal fluid (CSF) Aβ–3–40/Aβ42 ratio (95% CI: 0.753–0.981, black line), 0.873 for the Aβ42/Aβ40 ratio (95% CI: 0.750–0.997, blue line), and 0.880 for a model including both ratios, CSF Aβ–3–40/Aβ42 and Aβ42/Aβ40 (95% CI: 0.762–0.997, green line)

advantages compared to the established CSF measurements of Aβ42, Aβ1-42, or the CSF Aβ42/Aβ40 ratio (Alawode et al., 2021). Evidence of Aβ efflux from the central nervous system (CNS) to the blood by CSF and direct transport across the blood–brain barrier has been reported, and it was estimated to account for 50% of the clearance of CNS Aβ (Roberts et al., 2014). Thus, plasma Aβ is derived, at least in part, from brain but also from diverse peripheral sources including skeletal muscle, platelets, and vascular walls (Roher et al., 2009). Up to an estimated 30%–50% of plasma Aβ may originate from the CNS (Ovod et al., 2017).

Aβ–3–40 (APP669-711) is one out of 22 Aβ-related peptides that were detected in human blood plasma by IP-MS (Kaneko, Yamamoto, et al., 2014). Statistically significant differences in the plasma Aβ–3–40 concentration between amyloid PET-negative and amyloid PET-positive cases were not observed in two subsequent biomarker studies. However, plasma Aβ–3–40 turned out to represent a valuable reference to bring out the selective decrease in plasma Aβ1-42 in the amyloid PET-positive group by calculating the Aβ–3–40/Aβ1–42 ratio (Kaneko, Nakamura, et al., 2014; Nakamura et al., 2018). The origin of Aβ–3–40 in blood plasma is not clear, and, to the best of our knowledge, it has not been reported in previous mass spectrometric studies investigating the patterns of Aβ peptides in CSF (Portelius et al., 2007; Portelius, Westman-Brinkmalm, et al., 2006; Portelius, Zetterberg, et al., 2006; Vigo-Pelfrey et al., 1993). Aβ–3–40 can be produced in cell culture by Chinese hamster ovary 7PA2 cells (Portelius et al., 2013), BE(2)-C neuroblastoma cells (Nakamura et al., 2018) or SH-SY5Y cells transfected with wild-type APP (Beyer et al., 2016). The generation of Aβ variants N-terminally elongated by three amino acids (Aβ–3–x) appears to occur independently of BACE1 activity, as the abundance of Aβ–3–40 was found not to be reduced in cell culture models in the presence of BACE1 inhibitors (Beyer et al., 2016; Portelius et al., 2013). In a previous study and using antibodies directed against Aβ–3–x, we did not observe staining of extracellular amyloid plaques but only of surrounding dystrophic neurites in a transgenic mouse model of AD (Klafki et al., 2020). To the best of our knowledge, no such immunoreactivity has been described so far in plaques from post-mortem human AD brain. In general, the biophysical consequences of N-terminal elongations of Aβ peptides are largely unclear. It has been shown that N-terminally

elongated Aβ–3–38, Aβ–3–40, and Aβ–3–42 peptides can form β-sheet-rich fibrillar aggregates *in vitro* (Beyer et al., 2016). However, compared to Aβ1–42, the tendency of Aβ–3–40 to self-assemble was found to be lower (Nakamura et al., 2018). Others have shown that, in general, N-terminal elongations of 5–40 residues retard fibril formation of Aβ42 (Szczepankiewicz et al., 2015).

Here, we investigated whether Aβ–3–40 was also detectable in human CSF and if the CSF Aβ–3–40/Aβ42 ratio was able to differentiate between subjects with or without amyloid PET evidence of cerebral Aβ accumulation. Aβ–3–40 and Aβ–3–38 were clearly detected by mass spectrometry in immunoprecipitates from pooled lumbar CSF and from individual CSF samples from subjects with NPH. Thus, we conclude that N-terminally elongated Aβ–3–x peptides are normal constituents of human CSF. To quantify the CSF concentrations of Aβ–3–40 in 23 amyloid PET-negative and 17 amyloid PET-positive subjects, we employed an electrochemiluminescence sandwich immunoassay we have developed and validated previously (Klafki et al., 2020). In good agreement with the published observations in plasma (Kaneko, Nakamura, et al., 2014; Nakamura et al., 2018), we did not observe a statistically significant group difference in CSF Aβ–3–40, but a statistically significant increase in the Aβ–3–40/Aβ42 ratio in the amyloid PET-positive individuals. Comparison of ROC curves for single and combined biomarker candidates indicated that the selective decrease in CSF Aβ42 in amyloid PET-positive cases can apparently be accentuated by calculating the CSF Aβ–3–40/Aβ42 and Aβ42/Aβ40 ratios. Combining both CSF ratios to a composite biomarker resulted in a marginal increase in the area under the ROC curve. This observation, however, should be considered preliminary because of the small sample size, which is a clear limitation of the current study.

Taken together, we provide here, and to the best of our knowledge for the first time, unequivocal evidence of the presence of Aβ–3–40 in human CSF. There was no statistically significant difference in the level of CSF Aβ–3–40 between subjects with or without PET evidence of cerebral amyloid accumulation. In line with published findings in blood plasma, it appears that CSF Aβ–3–40 may serve as a reference to accentuate the selective decrease in CSF Aβ42 in amyloid PET-positive subjects. Further studies will be required to assess in more detail whether the CSF Aβ-3-40/Aβ42 ratio may provide an added value to the well-established CSF Aβ42/Aβ40 ratio as a neurochemical biomarker of AD. Future studies should preferably also include the assessment of correlations between CSF and plasma values.

ACKNOWLEDGEMENTS

We thank Gabriele Paetzold for expert technical help with sample preparation for mass spectrometry and Isaak Beyer and Hans-Joachim Knölker for providing synthetic Aβ-3-40. Furthermore, we greatly acknowledge Anke Jahn-Brodmann for her expert technical assistance. Jens Wiltfang is supported by an Ilídio Pinho professorship, iBiMED (UIDB/04501/2020) at the University of Aveiro, Portugal. Open access funding enabled and organized by ProjektDEAL.

CONFLICT OF INTEREST

The authors have no conflict of interest to report.

AUTHOR CONTRIBUTIONS

HWK and OJ designed the study, analyzed data and drafted the manuscript. OW analyzed data and contributed to the conception and design of the study and interpretation of findings. BM, JV and HE provided study material and contributed to the conception of the study and interpretation of the data. PR and TL performed experiments, acquired data and contributed to method development and optimization. JW provided study material and contributed to study design, interpretation of data and critical revision of the manuscript. All authors gave consent for publication.

DATA AVAILABILITY STATEMENT

The data that support the findings of this study are available from the corresponding author upon reasonable request.

ORCID

Hans-Wolfgang Klafki https://orcid.org/0000-0002-8672-9032
Oliver Wirths https://orcid.org/0000-0002-4115-0334
Brit Mollenhauer https://orcid.org/0000-0001-8437-3645
Hermann Esselmann https://orcid.org/0000-0001-5484-9710
Jonathan Vogelgsang https://orcid.org/0000-0001-9326-8193
Jens Wiltfang https://orcid.org/0000-0003-1492-5330
Olaf Jahn https://orcid.org/0000-0002-3397-8924

REFERENCES

Aichholzer, F., Klafki, H. W., Ogorek, I., Vogelgsang, J., Wiltfang, J., Scherbaum, N., Weggen, S., & Wirths, O. (2021). Evaluation of cerebrospinal fluid glycoprotein NMB (GPNMB) as a potential biomarker for Alzheimer's disease. *Alzheimer's Research & Therapy*, 13, 94.

Alawode, D. O. T., Heslegrave, A. J., Ashton, N. J., Karikari, T. K., Simrén, J., Montoliu-Gaya, L., Pannee, J., O´Connor, A., Weston, P. S. J., Lantero-Rodriguez, J., Keshavan, A., Snellman, A., Gobom, J., Paterson, R. W., Schott, J. M., Blennow, K., Fox, N. C., & Zetterberg, H. (2021). Transitioning from cerebrospinal fluid to blood tests to facilitate diagnosis and disease monitoring in Alzheimer's disease. *Journal of Internal Medicine*, 290, 583–601.

Alzheimer's Association (2021). 2021 Alzheimer's disease facts and figures. *Alzheimer Dementia*, 17, 327–406.

Ashton, N. J., Pascoal, T. A., Karikari, T. K., Benedet, A. L., Lantero-Rodriguez, J., Brinkmalm, G., Snellman, A., Scholl, M., Troakes, C., Hye, A., Gauthier, S., Vanmechelen, E., Zetterberg, H., Rosa-Neto, P., & Blennow, K. (2021). Plasma p-tau231: A new biomarker for incipient Alzheimer's disease pathology. *Acta Neuropathologica*, 141, 709–724.

Beyer, I., Rezaei-Ghaleh, N., Klafki, H. W., Jahn, O., Haussmann, U., Wiltfang, J., Zweckstetter, M., & Knolker, H. J. (2016). Solid-Phase synthesis and characterization of N-terminally elongated Abeta-3-x -peptides. *Chemistry*, 22, 8685–8693.

Blennow, K., & Zetterberg, H. (2018). The past and the future of Alzheimer's disease fluid biomarkers. *Journal of Alzheimer's Disease*, 62, 1125–1140.

Cummings, J. (2019). The role of biomarkers in Alzheimer's disease drug development. *Advances in Experimental Medicine and Biology*, 1118, 29–61.

Faul, F., Erdfelder, E., Lang, A. G., & Buchner, A. (2007). G*Power 3: A flexible statistical power analysis program for the social, behavioral, and biomedical sciences. *Behavior Research Methods*, 39, 175–191.

Haussmann, U., Jahn, O., Linning, P., Janssen, C., Liepold, T., Portelius, E., Zetterberg, H., Bauer, C., Schuchhardt, J., Knolker, H. J., Klafki, H., & Wiltfang, J. (2013). Analysis of amino-terminal variants of amyloid-beta peptides by capillary isoelectric focusing immunoassay. *Analytical Chemistry*, 85, 8142–8149.

Jack, C. R. Jr, Knopman, D. S., Jagust, W. J., Shaw, L. M., Aisen, P. S., Weiner, M. W., Petersen, R. C., & Trojanowski, J. Q. (2010). Hypothetical model of dynamic biomarkers of the Alzheimer's pathological cascade. *The Lancet. Neurology*, 9, 119–128.

Jagust, W. (2018). Imaging the evolution and pathophysiology of Alzheimer disease. *Nature Reviews Neuroscience*, 19, 687–700.

Janelidze, S., Mattsson, N., Palmqvist, S., Smith, R., Beach, T. G., Serrano, G. E., Chai, X., Proctor, N. K., Eichenlaub, U., Zetterberg, H., Blennow, K., Reiman, E. M., Stomrud, E., Dage, J. L., & Hansson, O. (2020). Plasma P-tau181 in Alzheimer's disease: Relationship to other biomarkers, differential diagnosis, neuropathology and longitudinal progression to Alzheimer's dementia. *Nature Medicine*, 26, 379–386.

Kaneko, N., Nakamura, A., Washimi, Y., Kato, T., Sakurai, T., Arahata, Y., Bundo, M., Takeda, A., Niida, S., Ito, K., Toba, K., Tanaka, K., & Yanagisawa, K. (2014). Novel plasma biomarker surrogating cerebral amyloid deposition. *Proceedings of the Japan Academy. Series B, Physical and Biological Sciences*, 90, 353–364.

Kaneko, N., Yamamoto, R., Sato, T. A., & Tanaka, K. (2014). Identification and quantification of amyloid beta-related peptides in human plasma using matrix-assisted laser desorption/ionization time-of-flight mass spectrometry. *Proceedings of the Japan Academy. Series B, Physical and Biological Sciences*, 90, 104–117.

Karikari, T. K., Pascoal, T. A., Ashton, N. J., Janelidze, S., Benedet, A. L., Rodriguez, J. L., Chamoun, M., Savard, M., Kang, M. S., Therriault, J., Schöll, M., Massarweh, G., Soucy, J.-P., Höglund, K., Brinkmalm, G., Mattsson, N., Palmqvist, S., Gauthier, S., Stomrud, E., … Blennow, K. (2020). Blood phosphorylated tau 181 as a biomarker for Alzheimer's disease: A diagnostic performance and prediction modelling study using data from four prospective cohorts. *The Lancet. Neurology*, 19, 422–433.

Klafki, H. W., Rieper, P., Matzen, A., Zampar, S., Wirths, O., Vogelgsang, J., Osterloh, D., Rohdenburg, L., Oberstein, T. J., Jahn, O., Beyer, I., Lachmann, I., Knolker, H. J., & Wiltfang, J. (2020). Development and technical validation of an immunoassay for the detection of APP669-711 (Abeta-3-40) in biological samples. *International Journal of Molecular Sciences*, 21, 6564.

Knobloch, M., Konietzko, U., Krebs, D. C., & Nitsch, R. M. (2007). Intracellular Abeta and cognitive deficits precede beta-amyloid deposition in transgenic arcAbeta mice. *Neurobiology of Aging*, 28, 1297–1306.

Kornhuber, J., Schmidtke, K., Frölich, L., Perneczky, R., Wolf, S., Hampel, H., Jessen, F., Heuser, I., Peters, O., Weih, M., Jahn, H., Luckhaus, C., Hüll, M., Gertz, H.-J., Schröder, J., Pantel, J., Rienhoff, O., Seuchter, S. A., Rüther, E., … Wiltfang, J. (2009). Early and differential diagnosis of dementia and mild cognitive impairment: design and cohort baseline characteristics of the German Dementia Competence Network. *Dementia and Geriatric Cognitive Disorders*, 27, 404–417.

Lewczuk, P., Kornhuber, J., & Wiltfang, J. (2006). The German competence net dementias: Standard operating procedures for the neurochemical dementia diagnostics. *Journal of Neural Transmission*, 113, 1075–1080.

Lord, A., Kalimo, H., Eckman, C., Zhang, X. Q., Lannfelt, L., & Nilsson, L. N. (2006). The Arctic Alzheimer mutation facilitates early intraneuronal Abeta aggregation and senile plaque formation in transgenic mice. *Neurobiology of Aging*, 27, 67–77.

Maler, J. M., Klafki, H. W., Paul, S., Spitzer, P., Groemer, T. W., Henkel, A. W., Esselmann, H., Lewczuk, P., Kornhuber, J., & Wiltfang, J. (2007). Urea-based two-dimensional electrophoresis of beta-amyloid peptides in human plasma: Evidence for novel Abeta species. *Proteomics*, 7, 3815–3820.

Munter, L. M., Botev, A., Richter, L., Hildebrand, P. W., Althoff, V., Weise, C., Kaden, D., & Multhaup, G. (2010). Aberrant amyloid precursor protein (APP) processing in hereditary forms of Alzheimer disease caused by APP familial Alzheimer disease mutations can be rescued by mutations in the APP GxxxG motif. *Journal of Biological Chemistry*, 285, 21636–21643.

Nakamura, A., Kaneko, N., Villemagne, V. L., Kato, T., Doecke, J., Dore, V., Fowler, C., Li, Q. X., Martins, R., Rowe, C., Tomita, T., Matsuzaki, K., Ishii, K., Ishii, K., Arahata, Y., Iwamoto, S., Ito, K., Tanaka, K., Masters, C. L., … Yanagisawa, K. (2018). High performance plasma amyloid-beta biomarkers for Alzheimer's disease. *Nature*, 554, 249–254.

Ovod, V., Ramsey, K. N., Mawuenyega, K. G., Bollinger, J. G., Hicks, T., Schneider, T., Sullivan, M., Paumier, K., Holtzman, D. M., Morris, J. C., Benzinger, T., Fagan, A. M., Patterson, B. W., & Bateman, R. J. (2017). Amyloid beta concentrations and stable isotope labeling kinetics of human plasma specific to central nervous system amyloidosis. *Alzheimer's & Dementia*, 13, 841–849.

Portelius, E., Olsson, M., Brinkmalm, G., Ruetschi, U., Mattsson, N., Andreasson, U., Gobom, J., Brinkmalm, A., Holtta, M., Blennow, K., & Zetterberg, H. (2013). Mass spectrometric characterization of amyloid-beta species in the 7PA2 cell model of Alzheimer's disease. *Journal of Alzheimer's Disease*, 33, 85–93.

Portelius, E., Tran, A. J., Andreasson, U., Persson, R., Brinkmalm, G., Zetterberg, H., Blennow, K., & Westman-Brinkmalm, A. (2007). Characterization of amyloid beta peptides in cerebrospinal fluid by an automated immunoprecipitation procedure followed by mass spectrometry. *Journal of Proteome Research*, 6, 4433–4439.

Portelius, E., Westman-Brinkmalm, A., Zetterberg, H., & Blennow, K. (2006). Determination of beta-amyloid peptide signatures in cerebrospinal fluid using immunoprecipitation-mass spectrometry. *Journal of Proteome Research*, 5, 1010–1016.

Portelius, E., Zetterberg, H., Andreasson, U., Brinkmalm, G., Andreasen, N., Wallin, A., Westman-Brinkmalm, A., & Blennow, K. (2006). An Alzheimer's disease-specific beta-amyloid fragment signature in cerebrospinal fluid. *Neuroscience Letters*, 409, 215–219.

Price, J. L., & Morris, J. C. (1999). Tangles and plaques in nondemented aging and "preclinical" Alzheimer's disease. *Annals of Neurology*, 45, 358–368.

Roberts, K. F., Elbert, D. L., Kasten, T. P., Patterson, B. W., Sigurdson, W. C., Connors, R. E., Ovod, V., Munsell, L. Y., Mawuenyega, K. G., Miller-Thomas, M. M., Moran, C. J., Cross, D. T. 3rd, Derdeyn, C. P., & Bateman, R. J. (2014). Amyloid-beta efflux from the central nervous system into the plasma. *Annals of Neurology*, 76, 837–844.

Roher, A. E., Esh, C. L., Kokjohn, T. A., Castano, E. M., Van Vickle, G. D., Kalback, W. M., Patton, R. L., Luehrs, D. C., Daugs, I. D., Kuo, Y. M., Emmerling, M. R., Soares, H., Quinn, J. F., Kaye, J., Connor, D. J., Silverberg, N. B., Adler, C. H., Seward, J. D., Beach, T. G., … Sabbagh, M. N. (2009). Amyloid beta peptides in human plasma and tissues and their significance for Alzheimer's disease. *Alzheimer's & Dementia*, 5, 18–29.

Schindler, S. E., Bollinger, J. G., Ovod, V., Mawuenyega, K. G., Li, Y., Gordon, B. A., Holtzman, D. M., Morris, J. C., Benzinger, T. L. S., Xiong, C., Fagan, A. M., & Bateman, R. J. (2019). High-precision plasma beta-amyloid 42/40 predicts current and future brain amyloidosis. *Neurology*, 93, e1647–e1659.

Shahpasand-Kroner, H., Klafki, H. W., Bauer, C., Schuchhardt, J., Huttenrauch, M., Stazi, M., Bouter, C., Wirths, O., Vogelgsang,

J., & Wiltfang, J. (2018). A two-step immunoassay for the simultaneous assessment of Abeta38, Abeta40 and Abeta42 in human blood plasma supports the Abeta42/Abeta40 ratio as a promising biomarker candidate of Alzheimer's disease. *Alzheimer's Research & Therapy*, 10, 121.

Szczepankiewicz, O., Linse, B., Meisl, G., Thulin, E., Frohm, B., Sala Frigerio, C., Colvin, M. T., Jacavone, A. C., Griffin, R. G., Knowles, T., Walsh, D. M., & Linse, S. (2015). N-terminal extensions retard Abeta42 fibril formation but allow cross-seeding and coaggregation with Abeta42. *Journal of the American Chemical Society*, 137, 14673–14685.

Vigo-Pelfrey, C., Lee, D., Keim, P., Lieberburg, I., & Schenk, D. B. (1993). Characterization of beta-amyloid peptide from human cerebrospinal fluid. *Journal of Neurochemistry*, 61, 1965–1968.

SUPPORTING INFORMATION

Additional supporting information may be found in the online version of the article at the publisher's website.

How to cite this article: Klafki, H.-W., Wirths, O., Mollenhauer, B., Liepold, T., Rieper, P., Esselmann, H., Vogelgsang, J., Wiltfang, J., & Jahn, O. (2022). Detection and quantification of Aβ–3–40 (APP669-711) in cerebrospinal fluid. *Journal of Neurochemistry*, 160, 578–589. https://doi.org/10.1111/jnc.15571